



threshold voltage ( $V_{to}=V_{th}$ ). Since this diode is forward biased, the gate node of drive TFT (DR) is *precharged* to the gate high voltage minus the TFT's threshold voltage ( $V_{GH}-V_{th}$ ) and stored in the first storage capacitor ( $C_{st1}$ ). During the compensate state, previous gate2 is turned off, whereas gate1 (Gate1[n]) and gate2 (Gate2[n]) are turned on, and the data signal ( $D[n]$ ) voltage  $V_d$  is applied to the source node of the mirror TFT (MR). The first switch TFT (SW1) connects the gate and drain of mirror TFT to form a diode with turn-on voltage equal to the TFT's threshold voltage ( $V_{to}=V_{th}$ ). Since  $V_{GH}-V_{th}$  was precharged in  $C_{ST1}$  during precharge state, and this voltage is higher than  $V_d$ , MR diode is forward biased. The gate node voltage of DR (or the anode voltage of MR) is decreased as  $C_{st1}$  is discharged by MR diode, which will converge to the data voltage plus the turn-on voltage of MR diode ( $V_d+V_{th}$ ).

Assuming that the threshold voltage of MR and DR is identical ( $V_{th_{DR}}=V_{th_{MR}}$ ), the voltage value now stored in  $C_{st1}$  will *compensate* the OLED current by canceling out the threshold voltage of DR, as shown in the following equations.

$$I_{OLED} = \frac{k}{2}(V_{GS} - V_{th_{DR}})^2, V_{GS} = V_d + V_{th_{MR}}$$

$$I_{OLED} = \frac{k}{2}(V_d + V_{th_{MR}} - V_{th_{DR}})^2 = \frac{k}{2}V_d^2$$

During the restore state, gate1 signal is turned off, whereas gate2 is still on, and the data signal voltage is 0V ( $Gnd$ ). While the gate voltage of DR and MR is held at  $V_d+V_{th}$ , the source voltage of MR is decreased from  $V_d$  to  $Gnd$ , and restored in the second storage capacitor ( $C_{st2}$ ). Our recent studies convey that when the gate-to-source voltage of both DR and MR is identical, the amount of threshold voltage shift due to gate bias stress should also be identical. This corresponds to the previous assumption that the threshold voltage of DR and MR is the same. During drive state, gate2 signal is finally turned off, and DR *drives* the compensated OLED current. SPICE simulation results verify that the proposed pixel circuit compensates the OLED

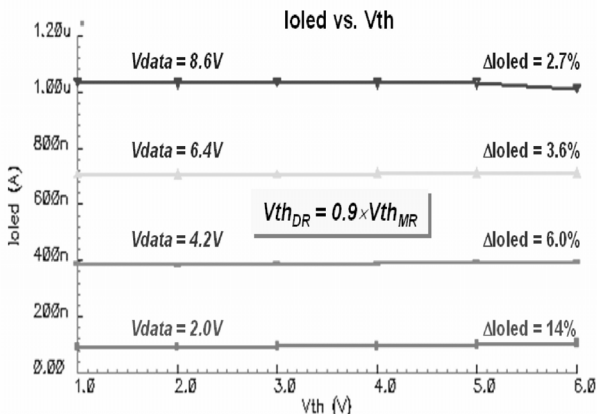


Figure 2 I<sub>OLED</sub> reduction as function of TFT's V<sub>th</sub> shift.

current reduction induced by TFT threshold voltage shift up to 5V, resulting in maximum OLED current reduction ( $= \Delta I_{OLED} / I_{OLED} [\%] = 4\Delta V_{th} / (V_{GS}-V_{th})$ ) of less than 14%, as shown in Figure 2.

### 2.2 Current-Driven Pixel Electrode Circuit

The proposed current-driven pixel electrode circuit [9] consists of two switching TFTs (T1 and T2), one mirror TFT (T4), one driving TFT (T3), and two storage capacitors ( $C_{ST1}$ ,  $C_{ST2}$ ) connected between a scan line and ground with a cascade structure, Figure 3.

The pixel circuit operation mechanism can be described as follow: During the ON-state,  $V_{SCAN}$  turns on the T1 and T2, and  $I_{DATA}$  ( $=I_{OLED-ON}$ ) passes through T1 and T4 shown as the solid line in Fig. 4, and sets up the voltage at T2 drain electrode (node  $V_A$ ). At the same time, the voltage at T4 gate electrode (node  $V_B$ ) is set by  $I_{DATA}$  passing through T4. Since  $I_{DATA}$  is current source, the gate voltage of T4 is automatically set high enough to allow the fixed  $I_{DATA}$  flowing through T1 and T4. In the pixel simulation, since the current-scaling is not controlled by the geometry ratio of the transistors, T3 and T4 are designed as having the same geometries. Since in the ideal case T3 and T4 are assumed identical and the gate bias ( $V_{B\_ON}$ ) is common to both TFTs, the same amount of current ( $I_{DATA}$ ) is expected to flow through OLED to T3 by  $V_{DD}$ . The  $V_{B\_ON}$  will be stored in both  $C_{ST1}$  and  $C_{ST2}$ , and the voltage across  $C_{ST2}$  is  $V_{SCAN} - V_{B\_ON}$ . When the pixel changes from the ON- to OFF-state,  $V_{SCAN}$  turns off T1 and T2. Because  $C_{ST2}$  is connected between the scan line and the node B to form a cascade structure with  $C_{ST1}$ , the change of  $V_{SCAN}$  will reduce  $V_{B\_ON}$  to  $V_{B\_OFF}$  due to the feed-through effect of the capacitors.  $V_{B\_OFF}$  can be derived from the charge conservation theory as  $V_{B\_OFF} = V_{B\_ON} - \Delta V_{SCAN} \cdot C_{ST2} / (C_{ST1}+C_{ST2})$ .

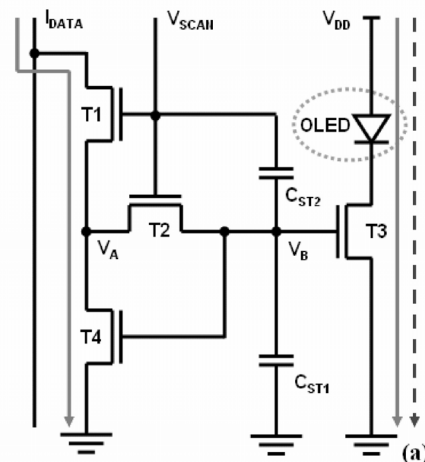


Figure 3 Schematic diagram of proposed current-driven pixel circuit [9].

A reduced T3 gate voltage ( $V_{B\_OFF}$ ) will be held in  $C_{ST1}$  and  $C_{ST2}$  and it will continuously turn on T3 during the OFF-state. Since gate bias of T3 ( $V_{B\_ON}$ ) is reduced to  $V_{B\_OFF}$  by the ratio of cascaded capacitor, a scaled-down data current ( $I_{OLED\_OFF}$ ) from  $I_{OLED\_ON}$  by ratio of  $C_{ST2}/C_{ST1}$  will flow through OLED, shown as the dashed line in Figure 4. Consequently, when a very large data current ( $I_{DATA}$ ) can be used to charge the pixel electrode to shorten the pixel programming time, a smaller driving current ( $I_{OLED\_OFF}$ ) can be achieved for lower gray scales at the same time. To investigate the current scaling ratio of the proposed pixel electrode circuit, we changed the  $I_{DATA}$  from 0.2 to 5  $\mu A$  and measured the corresponding  $I_{OLED\_ON}$  and  $I_{OLED\_OFF}$  flowing through the diode for different ratios of cascaded-capacitors. In ON-state, the  $I_{OLED\_ON}$  is identical to the data current ( $I_{DATA}$ ), Figure 4. When the pixel circuit operates in OFF-state, the diode current ( $I_{OLED\_OFF}$ ) is scaled-down by the ratio of cascade capacitor as discussed above. From Figure 4, it is obvious that the larger  $C_{ST2}/C_{ST1}$  results in significant decrease of the  $I_{OLED\_OFF}$  at lower  $I_{DATA}$ . In the proposed pixel circuit, since  $I_{OLED\_ON}$  is not affected by the threshold voltage variation, the variation of  $I_{OLED\_OFF}$  with  $\Delta V_{TH}$  is used to estimate its influence on the performance of pixel circuit. For

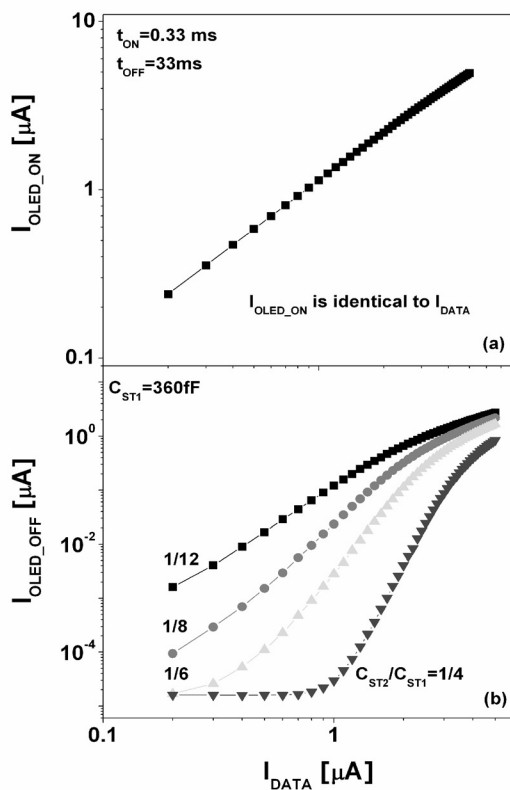


Figure 4 Variation of the simulated  $I_{OLED\_ON}$ ,  $I_{OLED\_OFF}$ , and  $I_{AVE}$  as a function of  $I_{DATA}$  for various  $C_{ST2}/C_{ST1}$  ratios.

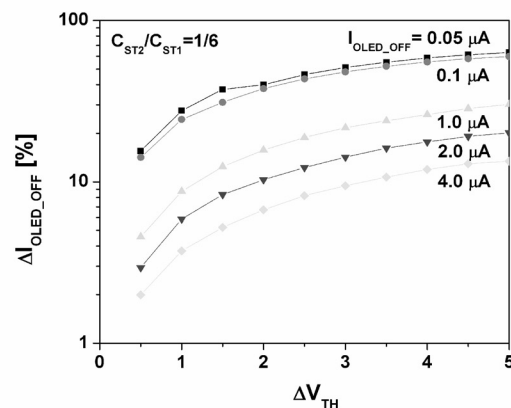


Figure 5 Variation of  $\Delta I_{OLED\_OFF}$  as a function of TFT threshold voltage shift.

given  $C_{ST2}/C_{ST1}$ , the variation of the  $I_{OLED\_OFF}$  with the  $\Delta V_{TH}$  can be defined by,

The variation of  $I_{OLED\_OFF}$  as a function of the  $\Delta V_{TH}$  is

$$\Delta I_{OLED\_OFF} = \frac{I_{OLED\_OFF}(\Delta V_{TH}) - I_{OLED\_OFF}(\Delta V_{TH} = 0)}{I_{OLED\_OFF}(\Delta V_{TH} = 0)}$$

shown in Figure 5. It should be noted that this  $\Delta I_{OLED\_OFF}$  increase corresponds to overall reduction of  $I_{OLED\_OFF}$  with the increase of  $\Delta V_{TH}$ . As  $\Delta V_{TH}$  increases up to 5V,  $\Delta I_{OLED\_OFF}$  also increases from 4 to 25% when  $I_{OLED\_OFF}$  is higher than 1.0  $\mu A$ ; a larger increase of  $\Delta I_{OLED\_OFF}$  is observed when  $I_{OLED\_OFF}$  is lower than 100nA. From our data, we can conclude that a large  $C_{ST2}/C_{ST1}$  can achieve a high  $R_{SCALE}$  but will also result in a large  $\Delta I_{OLED\_OFF}$ .

### 2.3 Driving a-Si:H TFT Structures

As discussed above, the pixel circuit performance is very sensitive to  $V_{TH}$  variation of driving a-Si:H TFTs. Therefore, suppressing device  $V_{TH}$  variation is the key to the future success of AM-OLEDs. Since a-Si:H TFT  $V_{TH}$  variation is mainly originated from a high gate bias [10] to supply a high OLED current, it is possible to reduce the gate bias level by using TFTs with larger channel width. However, due to reduction of pixel electrode aperture ratio, conventional TFT structure can not be enlarged enough to provide adequate level of OLED current. Alternatively, an interdigitated or fork-shaped TFT with a large channel width has been proposed for AM-OLEDs [11], Figure 6. However, it is known that a single transistor with a larger channel width results in a larger TFT threshold voltage shift in comparison with the normal (switching type) TFT [12], which was also experimentally verified in our laboratory. To address this critical problem, we propose, for example, Corbino a-Si:H TFT as driving device for AM-OLEDs [13], Figure 7. The Corbino a-Si:H TFT is composed of circle-shape inner electrode and ring-shaped

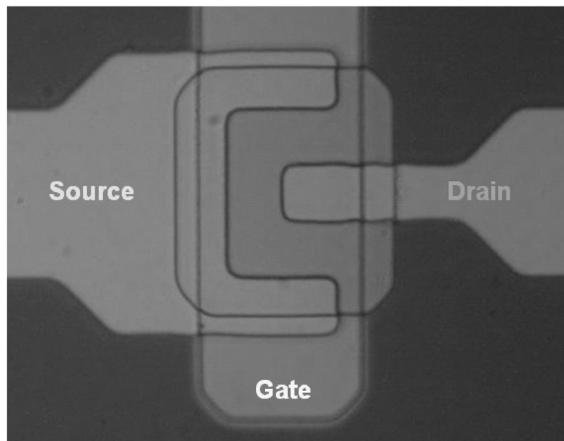


Figure 6 Top view of Fork a-Si:H TFT.

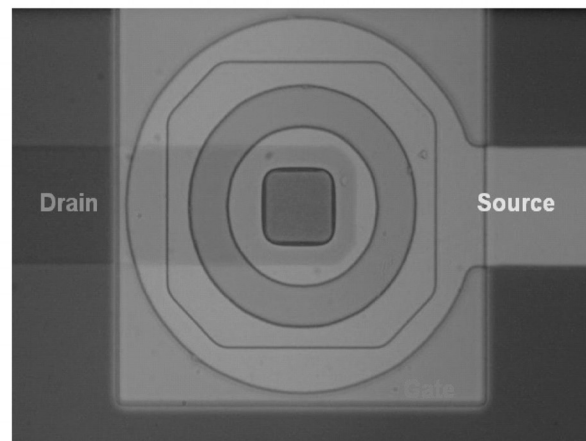


Figure 7 Top view of Corbino a-Si:H TFT.

outer electrode. Since the ring-shaped electrode provides a uniform electric field distribution in the channel and eliminates any local electric-field crowding due to sharp corners present in normal TFT, Corbino TFT shows better electrical stability even for larger W/L ratio in comparison to normal TFTs. Therefore, Corbino a-Si:H TFT is a good candidate to be used as a driving TFT for top light-emitting anode AM-OLEDs. Figure 8 shows an example of pixel circuit including driving Corbino a-Si:H TFT.

### 3. CONCLUSION

We described new a-Si:H TFT pixel circuits suitable for enhancing the electrical reliability of AM-OLED. Proposed pixel circuits are composed of a-Si:H TFTs and top-anode OLED structure. By using SPICE simulations, we verified that the voltage-driven circuit does not require any complicated drive ICs to compensate for OLED current reduction due to the TFT threshold voltage shift. In the current-driven circuit, by employing the cascaded capacitors connected to the driving TFT, we produce better non-linear scaling-function than the cascade capacitor circuit, which has a high scaling ratio at low current levels and a low scaling ratio at high current levels. Further more, by using novel Corbino a-Si:H TFTs as a driving TFT, the pixel electrode circuit electrical stability is further enhanced, which relax stability demands on pixel circuits. The pixel design value  $[\mu\epsilon_{ox}W/(2t_{ox}L)]$  must be very carefully chosen to satisfy both spatial and temporal reliability requirements of the AM-OLEDs.

This research was supported by R & D Center of LG Philips LCD, Korea.

### REFERENCE

1. J. Sanford and F. Libsch, *SID 03 Digest*. (2003) 13.
2. J. C. Goh, J. Jang, K. S. Cho, and C. K. Kim: *IEEE Electron Device Lett.* **24** (2003) 583.
3. J. H. Lee, J. H. Kim, and M. K. Han: *IEEE*

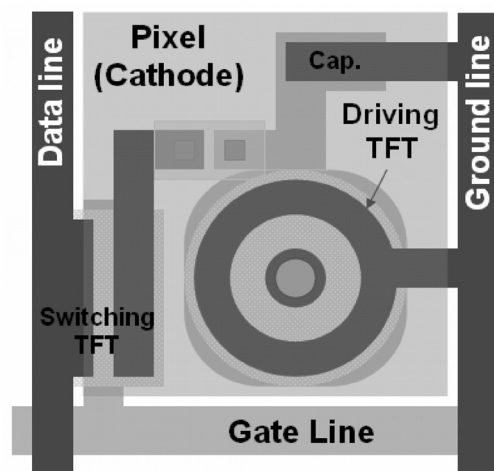


Figure 8 Top view of Corbino a-Si:H TFT for AM-OLED.

- Electron Device Lett.* **26** (2005) 897.
4. H. S. Shin, J. H. Lee, K. S. Shin, and M. K. Han: in *Proc. IDW* (2005) 657.
5. A. Yumoto, M. Asano, H. Hasegawa, and M. Sekiya: *Proc. Int. Display Workshop* (2001) 1395.
6. S. Ono and Y. Kobayashi: *IEICE Trans. Electron.* E88-C (2005) 264.
7. Y. C. Lin, H. P. D. Shieh, and J. Kanicki: *IEEE Trans. Electron Devices* **52** (2005) 1123.
8. J. S. Yoo, H. Lee, J. Kanicki, C. D. Kim and I. J. Chung: *Proc. Int. Display Research Conf.* (2006).
9. H. Lee, J. S. Yoo, C- D. Kim, I- J. Chung, and J. Kanicki: *Journal of Jpn. Appl. Phys.* **46** (2007) 1343.
10. A. Kuo and J. Kanicki: *Digest of Technical Papers AM-FPD*, (2006) 39.
11. H. Lee, J. S. Yoo, C. D. Kim, I. B. Kang, and J. Kanicki: *to be published*.
12. K- S. Shin, J- H. Lee, W- K. Lee, S- G. Park, and M- K. Han: *Mater. Res. Soc. Symp. Proc.* **910** (2006) 0910-A22-02.
13. H. Lee, J. S. Yoo, C.D. Kim, I. J. Chung, and J. Kanicki: *IEEE Trans. Electron Devices* **54** (2007) 654.